Deposition temperature effect of RF magnetron sputtered molybdenum oxide films on the power conversion efficiency of bulk-heterojunction solar cells

2011 J. Phys. D: Appl. Phys. 44 045101

(http://iopscience.iop.org/0022-3727/44/4/045101)

IOP PUBLISHING JOURNAL OF PHYSICS D: APPLIED PHYSICS

J. Phys. D: Appl. Phys. **44** (2011) 045101 (6pp) doi:10.1088/0022-3727/44/4/045101

Deposition temperature effect of RF magnetron sputtered molybdenum oxide films on the power conversion efficiency of bulk-heterojunction solar cells

Xi Fan, Guojia Fang, Pingli Qin, Nanhai Sun, Nishuang Liu, Qiao Zheng, Fei Cheng, Longyan Yuan and Xingzhong Zhao

Key Laboratory of Artificial Micro- and Nano-structures of Ministry of Education, Department of Electronic Science and Technology, School of Physics and Technology, Wuhan University, Wuhan, 430072, People's Republic of China

E-mail: gjfang@whu.edu.cn

Received 6 August 2010, in final form 21 November 2010
Published 6 January 2011
Online at stacks.iop.org/JPhysD/44/045101

Abstract

We have reported efficient bulk-heterojunction (regioregular poly (3-hexylthiophene) : (6,6)-phenyl C_{61} butyric acid methyl ester (P3HT : PCBM)) solar cells with MoO_3 as a hole-selective layer deposited at different substrate temperatures from 100 °C to 400 °C by radio-frequency magnetron sputtering. The structure, morphology, optical and electrical properties of the MoO_3 films deposited at different substrate temperatures are also investigated. MoO_3 thin films deposited at 200 °C and below are amorphous in nature. However, the films deposited at 300 °C and 400 °C exhibit the presence of monoclinic Mo_9O_{26} and orthorhombic MoO_3, respectively. The electrical resistivity values of the MoO_3 thin films are close to each other from 100 to 300 °C and decrease from 2.7×10^6 to $2.6 \times 10^5\ \Omega$ cm with increasing substrate temperature from 300 to 400 °C. X-ray photoelectron spectroscopy core level analysis reveals the presence of Mo^{6+} oxidation state only in the films. We found that the optical band gap of MoO_3 has reduced from 3.82 to 3.67 eV with decreasing substrate temperature from 400 to 100 °C. This decrease in band gap reduces the potential barrier between FTO and P3HT : PCBM, leading to an increase in the short circuit photocurrent density from 8.51 mA cm^{-2} to 9.50 mA cm^{-2} and an increase in efficiency of ∼20.7%.

(Some figures in this article are in colour only in the electronic version)

1. Introduction

Molybdenum oxide (MoO_3) has been widely used in recent years in bulk-heterojunction (BHJ) solar cells as an electron-blocking and hole-selective layer to replace poly(3,4-ethylenedioxythiophene) : poly (styrenesulfonate) (PEDOT : PSS) [1–3]. Recently, the electronic structure of MoO_3 thin film has been investigated [4, 5]. However, in the fabrication process of electronic and optoelectronic oxide semiconductor devices, it is necessary to know the roles played by MoO_3 in the device as well as the physics and chemistry at the anode/MoO_3/BHJ interfaces/cathode devices. In our study, it is seen that MoO_3 has a band structure well suited for poly (3-hexylthiophene) : (6,6)-phenyl C_{61} butyric acid methyl ester (P3HT : PCBM) BHJ solar cells and provides an ohmic contact to P3HT. In recent years, many methods have been employed to deposit molybdenum oxide films such as thermal evaporation [1], radio-frequency (RF) magnetron sputtering [6], pulsed-laser deposition (PLD) [7], sol–gel deposition [8, 9] and chemical vapour deposition [10]. Among them, thermal evaporation has been used most widely to prepare MoO_3 films for BHJ solar cells. We select magnetron sputtering instead of thermal evaporation because the film properties can be optimized through various deposition process parameters such as O_2 partial pressure in the mixture gas, total pressure, substrate temperature and sputtering power

[6, 11–13]. To the best of our knowledge, MoO_3 films deposited by RF magnetron sputtering have been rarely reported for BHJ solar cells. In our work, we report the strong effect of MoO_3 deposition temperature on the current–voltage (J–V) characteristics of BHJ solar cells, and show that with decreasing deposition temperature from 400 to 100 °C, the short circuit current density (J_{SC}) of the BHJ solar cells increases from 8.51 to 9.50 mA cm^{-2}, and the power conversion efficiency (PCE) increases from 2.71% to 3.27%. To understand the effect of the MoO_3 thin films at different substrate temperatures on the PCE, the structure, morphology, optical and electrical properties of the MoO_3 films were necessarily investigated. Mo oxidation states in the films were given by x-ray photoelectron spectroscopy (XPS). Fluorinated tin oxide (FTO)/MoO_3/P3HT : PCBM/Al structure device was fabricated to confirm its potential device applications.

2. Experimental details

Molybdenum oxide thin films were deposited on fused silica substrates at different substrate temperatures ranging from 100 to 400 °C by RF magnetron sputtering from a Mo metal target. The thin films were deposited at a relative oxygen partial pressure $O_2/(Ar + O_2)$ of 50% without post-deposition annealing. The base pressure of the deposition chamber was below 10^{-4} Pa. All the films were deposited at a total pressure of 0.5 Pa and a RF power of 130 W. Before deposition, the target was pre-sputtered for 10 min to remove some possible contaminants. The MoO_3 thin films were deposited on fused silica substrates for 20 min. After one day, the compositions and chemical states of the molybdenum oxide films were examined by XPS (XSAM800).

As for the BHJ solar cell fabrication, first, a 10 ± 1 nm MoO_3 layer was deposited on FTO substrates at different substrate temperatures from 100 to 400 °C. Then, the solution of P3HT : PCBM (20 mg : 20 mg) in chlorobenzene (1.0 ml) was deposited by spin coating at 1000 rpm on the MoO_3 layer. Afterwards, Al electrodes (∼100 nm) were deposited on the P3HT : PCBM layer (∼150 nm) via thermal evaporation at a pressure of 10^{-4} Pa. The active area of device was 0.2 cm^2. Finally, the devices were annealed at 150 °C for 8 min under argon atmosphere (<1 ppm O_2 and <1 ppm H_2O). The film thickness was measured by a surface profile meter (Talysurf Series II). The electrical resistivity (ρ) of the film was obtained using a Keithley 4200 semiconductor characterization system at room temperature. The crystal structure of the film was characterized by x-ray diffraction (XRD, Bruker Axs, D8Advance) using Cu Kα radiation at 40 kV and 40 mA. The spectral transmittances of the molybdenum oxide thin films were recorded using a UV–VIS–NIR spectrophotometer. The morphology of MoO_3 deposited on the FTO substrates was characterized by atomic force microscopy (AFM, SPM-9500J3, Shimadzu, Japan). Photo-energy conversion characterization was recorded by a source meter (Model 2400, Keithley Instruments Inc., USA) under an illumination intensity of 100 mW cm^{-2} (Oriel 91192, AM 1.5, Global). From this, the performance parameters of the devices were calculated.

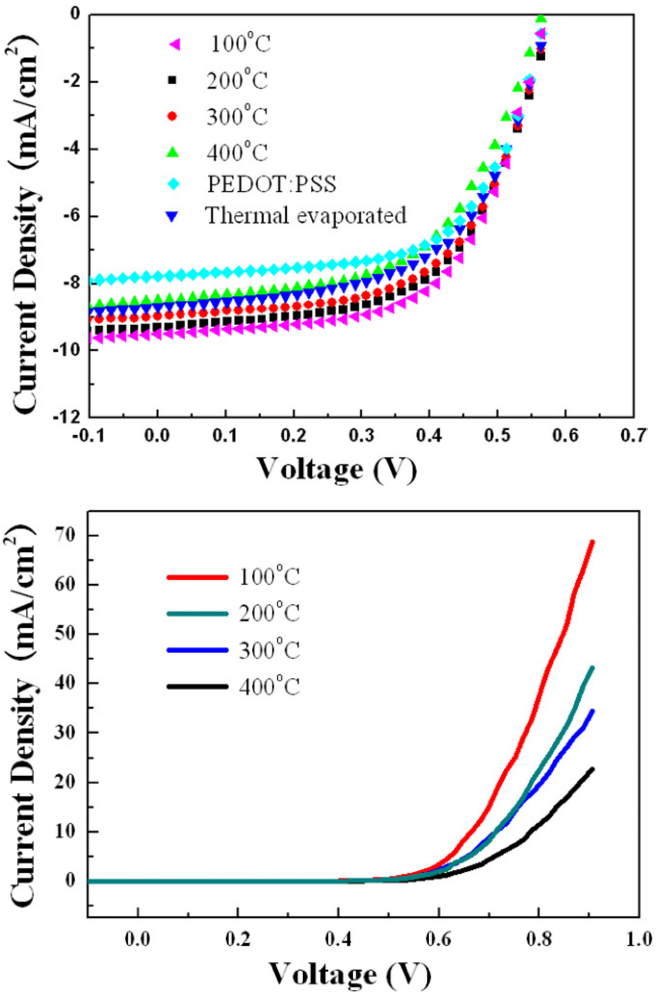

Figure 1. Light (top) and dark (bottom) J–V characteristics of the FTO/PEDOT : PSS/P3HT : PCBM/Al and the FTO/MoO_3/P3HT : PCBM/Al devices corresponding to different substrate temperature deposited MoO_3 films. A comparison of solar cells: (1) PEDOT : PSS: PCE = 2.74%, FF = 0.62, J_{SC} = 7.78 mA cm^{-2}, (2) evaporated MoO_3: PCE = 2.89%, FF = 0.58, J_{SC} = 8.68 mA cm^{-2}, (3) 100 °C: PCE = 3.27%, FF = 0.60, J_{SC} = 9.50 mA cm^{-2}, (4) 200 °C: PCE = 3.12%, FF = 0.59, J_{SC} = 9.31 mA cm^{-2}, (5) 300 °C: PCE = 2.95%, FF = 0.58, J_{SC} = 8.98 mA cm^{-2}, (6) 400 °C: PCE = 2.71%, FF = 0.57, J_{SC} = 8.51 mA cm^{-2}.

3. Results and discussion

Figure 1 shows the light (top) and dark (bottom) J–V characteristics for the solar cell devices with MoO_3 deposited at different substrate temperatures from 100 to 400 °C and the optimized PEDOT : PSS (∼30 nm) by adjusting the speed of spin coating under simulated 100 mW cm^{-2} (AM 1.5G) solar irradiation. In this study, the devices show power conversion efficiencies of 3.27% and 3.12% at 100 °C and 200 °C, respectively, exhibiting a higher performance which is much higher than that of the devices with a PEDOT : PSS layer and an evaporated MoO_3 layer. Hence, MoO_3 prepared by RF magnetron sputtering is quite suitable for fabricating BHJ solar cells as an electron-blocking and hole-selective layer. Specially, it also shows that J_{SC} increases from 8.51 to 9.50 mA cm^{-2} with decreasing substrate temperature from

Table 1. E_g, ρ and growth rate of molybdenum oxide films deposited at various substrate temperatures and the corresponding bulk solar cell performances.

T (°C)	100	200	300	400
E_g (eV)	3.67 ± 0.01	3.64 ± 0.01	3.72 ± 0.01	3.82 ± 0.01
ρ (Ω cm)	4.8×10^6	8.1×10^6	2.7×10^6	2.6×10^5
Growth rate (nm min^{-1})	6.25	7.75	10	9.25
J_{SC} (mA cm^{-2})	9.50	9.31	8.98	8.51
PCE (%)	3.27	3.12	2.95	2.71

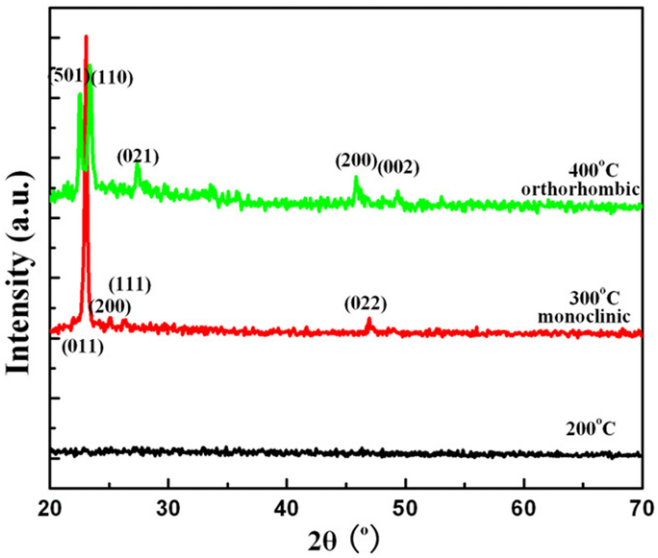

Figure 2. XRD patterns of the molybdenum oxide thin films deposited on fused silica substrates at different substrate temperatures from 100 to 400 °C.

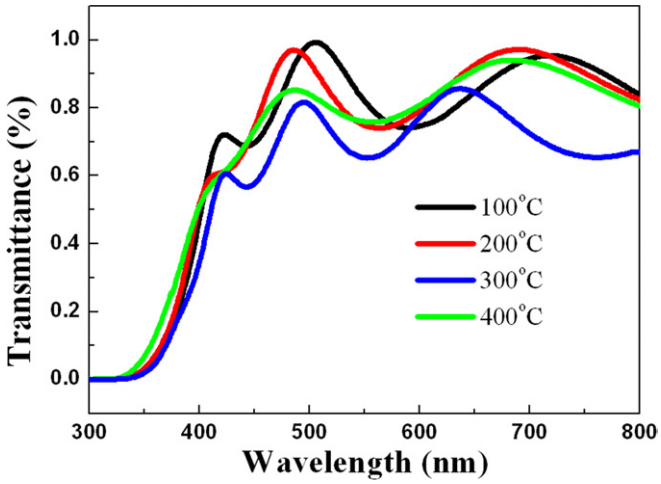

Figure 3. Transmittance spectra of the molybdenum oxide films deposited at different substrate temperatures from 100 to 400 °C for 40 min.

400 to 100 °C. This trend is supported by the dark J–V curves in which the device exhibited a higher rectification ratio with decreasing deposition temperature, indicating the better hole injection and electron-blocking properties. For comparison, the performance parameters are shown in table 1.

The XRD patterns of the MoO_3 films deposited on fused silica substrates at different substrate temperatures are shown in figure 2. Amorphous films were obtained below 200 °C. This can be attributed to the fact that crystallization and crystal lattice orientation of molybdenum oxide are not initiated on the fused silica substrates at low temperatures. When the substrate temperature increases to 300 and 400 °C, the crystalline nature of the films is observed, owing to the perfect growth alignment of MoO_3. The thin films deposited at 300 and 400 °C show the presence of monoclinic Mo_9O_{26} and orthorhombic MoO_3 with space groups $P21/c$ (14) and $Pbnm$ (62), respectively, which was also reported similarly in the literature by the same method of RF magnetron sputtering [6]. At a higher substrate temperature, the sputtering process may yield more active oxygen species due to the plasma decomposition of O_2 than that at a lower temperature [14].

The average grain sizes of the films deposited at 300 and 400 °C are calculated using the following Debye–Scherrer equation [15]:

$$D_{hkl} = \frac{0.9\lambda}{\beta_{hkl} \cos \theta_{hkl}},$$

where λ is the x-ray wavelength, θ_{hkl} is the Bragg diffraction angle and β_{hkl} is the full-width at half-maximum (FWHM) in radians of the main peak in the XRD patterns. The particle sizes are found to be 32 nm and 25 nm for the films deposited at 300 °C and 400 °C, respectively. The result confirms the presence of crystallites in the MoO_3 films prepared in this work.

Figure 3 presents the spectral transmittances of the MoO_3 thin films as a function of substrate temperature. The thicknesses of the molybdenum oxide films deposited at 100 °C, 200 °C, 300 °C and 400 °C are about 250 nm, 310 nm, 400 nm and 370 nm, respectively. The films deposited at lower temperatures are relatively thinner and their transmittances are relatively higher for the same deposition time.

The total absorption coefficient α was calculated from transmittance measurements with the aid of the expression [16]

$$\alpha = \ln \frac{I}{I_0} = \frac{1}{d} \ln \frac{1}{\mathrm{T}},$$

where d is the thickness of the MoO_3 film and T is the transmittance of the film. Figure 4 presents the variation of square of $(\alpha h\nu)^2$ versus photon energy ($h\nu$) for the MoO_3 films deposited at different temperatures. The optical band gap energies (E_g) are evaluated from the Tauc plot and are found to be 3.67 ± 0.01 eV, 3.64 ± 0.01 eV, 3.72 ± 0.01 eV and 3.82 ± 0.01 eV for the films deposited at 100 °C, 200 °C, 300 °C and 400 °C respectively, depending on the structural morphologies and crystal defects. The optical band gap calculated from the absorption data varies between 3.64 eV and 3.82 eV, which is in good agreement with the previous works [17, 18]. The direct band gap energy increases with an increase in substrate temperature, which might be attributed to the reduction of oxygen deficiency and the stoichiometric

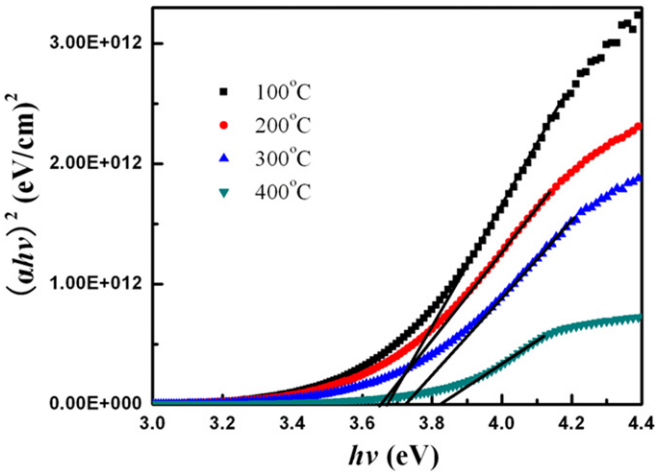

Figure 4. The dependence of $(\alpha h\nu)^2$ on $h\nu$ for molybdenum oxide thin films deposited at different temperatures.

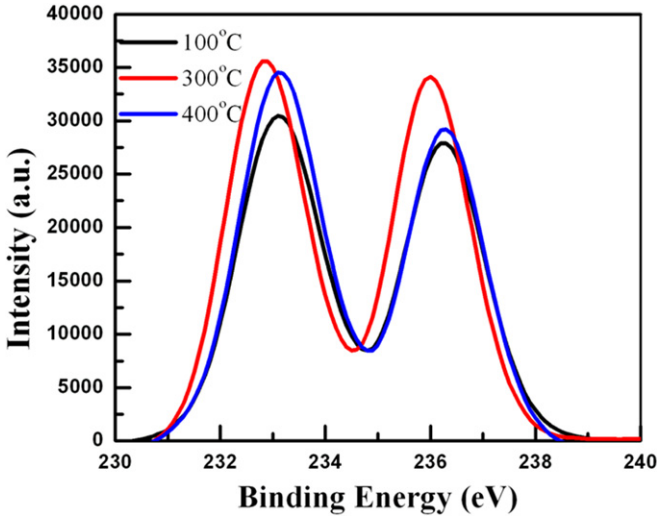

Figure 5. XPS spectra of MoO_3 deposited at 100 °C, 300 °C and 400 °C, respectively.

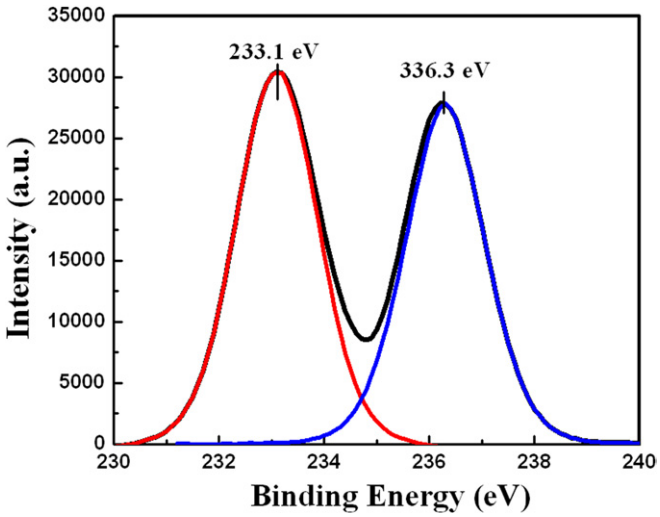

Figure 6. Core level spectra of MoO_3 film showing the presence of Mo^{6+} oxidation state, only.

approach of film composition [18]. At a higher substrate temperature, the sputtering process may yield more active oxygen species due to the plasma decomposition of O_2 than that at a lower temperature [14]. With the precise analysis of crystalline phase of XRD PDF cards, it is found that the thin films, annealed at 300 and 400 °C, exhibit the presence of monoclinic Mo_9O_{26} and orthorhombic MoO_3, respectively. The impurity energy state induced by oxygen deficiency might lead to a decrease in the band gap of MoO_3.

We also reckon that there are some relationships between the band gap and the structures. Amorphous, monoclinic and orthorhombic molybdenum oxides have different atomic arrangements. The slight difference between the two band gaps (3.67 ± 0.01 eV, 3.64 ± 0.01 eV) is possibly due to the same amorphous phase.

Table 1 also illustrates the growth rate of the molybdenum oxide films deposited at various substrate temperatures from 100 to 400 °C. The growth times of MoO_3 films are all the same, about 40 min at different substrate temperatures. It is observed that the growth rate of the molybdenum oxide films almost increases linearly with increasing substrate temperature except at 300 °C. The electrical resistivity of the MoO_3 films deposited at different substrate temperatures is also shown in table 1. It is obvious that the thin films exhibit a lower electrical resistivity at 400 °C, indicating the semiconducting nature of the films, and this may be also due to thermal excitation, impurities and lattice defects. The resistivity of the MoO_3 films increases from 2.6×10^5 to 2.7×10^6 Ω cm with decreasing substrate temperature from 400 to 300 °C, which is much lower than the previous reports ($>10^9$ Ω cm) [6, 19, 20]. But the resistivity values are close to each other from 100 to 300 °C in our experiment, which indicates that the change in PCE has not resulted from the electrical resistivity of the MoO_3 films.

The XPS spectra of the MoO_3 thin films deposited on silicon substrates at 100 , 300 and 400 °C are shown in figure 5. The binding energy of Mo 3d at 300 °C shifts to lower energies by about 0.2 eV as compared with those of MoO_3 deposited at 100 and 400 °C, due to electrostatic charging of the sample [21]. The core level spectrum consists of two peaks located at 232.6 ± 0.2 eV and 235.8 ± 0.2 eV, which corresponds to the Mo $3d_{3/2}$ and Mo $3d_{5/2}$ orbitals, respectively [22]. Figure 6 shows that the core level spectrum of MoO_3 deposited at 100 °C consists of two perfect Gaussian peaks located at 233.1 and 236.3 eV, which illustrates the presence of Mo^{6+} oxidation state only [22], due to the lower concentration of O vacancies or full reaction between Mo and O_2. And we found that the curves are very symmetrical like the curves in the literature [21, 22] and it is difficult to observe Mo^{4+} and Mo^{5+} states from 100 to 400 °C, which can eliminate the effect of Mo state on the PCE.

The surface morphologies of the FTO substrate and MoO_3 films deposited at different temperatures are compared in figure 7. The RMS of FTO is ∼15.55 nm. With decreasing deposition temperature from 400 to 100 °C, the RMS of the MoO_3 film gradually decreases from ∼13.72 to ∼10.13 nm. The roughness of polycrystalline MoO_3 films at higher deposition temperatures is higher than that of amorphous MoO_3 films at lower deposition temperatures, mainly due to the formation of crystalline MoO_3 particles. The slight difference in RMS results might have an effect on the performance parameters of solar cells but it is very limited. Further detailed

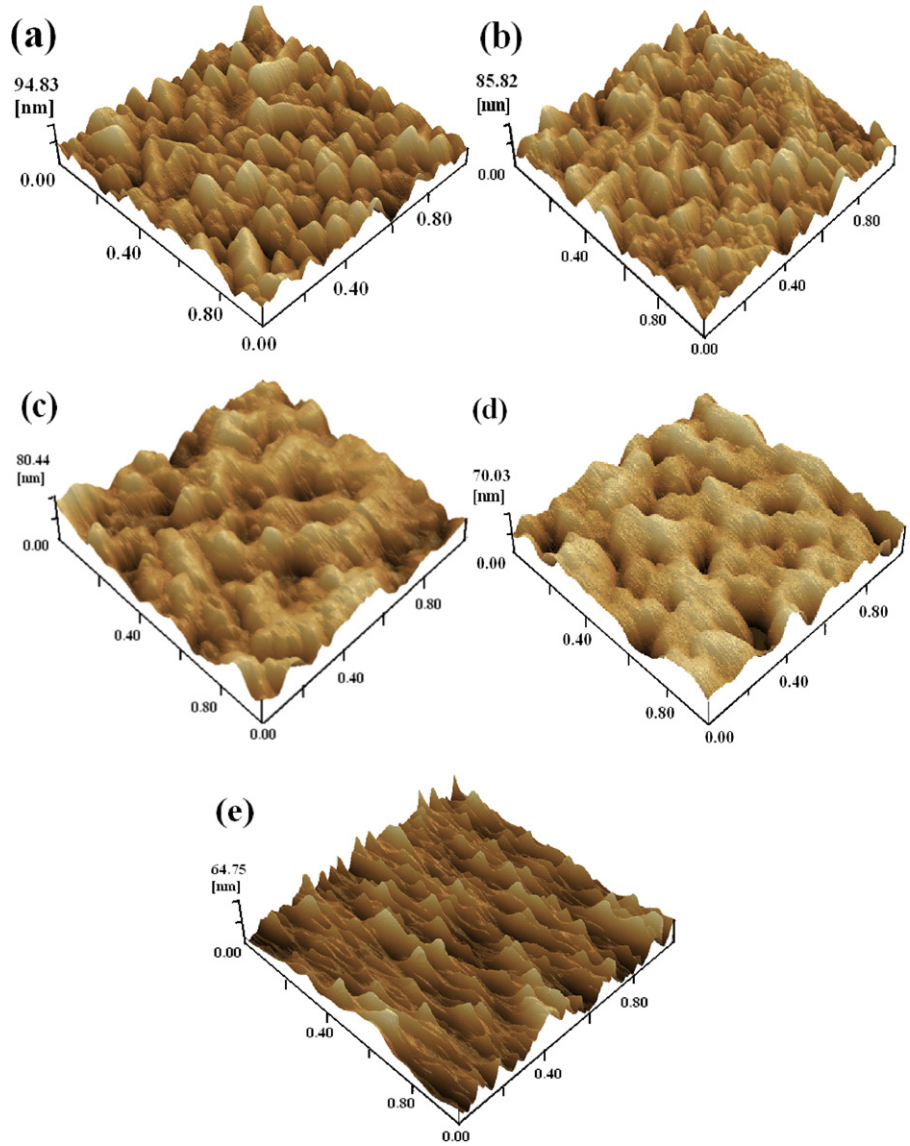

Figure 7. The morphologies of FTO substrate and MoO_3 films deposited at different temperatures from 400 to 100 °C. (*a*) FTO: 15.55 nm; (*b*) MoO_3 400 °C: 13.72 nm; (*c*) 300 °C: 12.65 nm; (*d*) 200 °C: 11.44 nm; (*e*) 100 °C: 10.13 nm. AFM height images of devices showing 1.00 μm × 1.00 μm surface areas.

studies on the link between the performance parameters and RMS are in progress.

Thus, J_{SC} and PCE seem to be roughly correlated with the optical band gap, although the effect of other characteristics of the MoO_3 film on the BHJ morphology could account for such differences. In the FTO/MoO_3/P3HT : PCBM/Al structure devices, the MoO_3 layer is a hole-selective and electron-blocking layer as shown in figure 8. Due to the fact that the lowest unoccupied molecular orbital (LUMO) of P3HT is much lower than the energy level of the conduction band (CB) of MoO_3, which significantly blocks the electron transfer to MoO_3, the discrepancy of J_{SC} does not arise from the transfer and collection of electrons by the Al cathodes. Hole injection has an effect on J_{SC}. It can be assumed that the position of CB is invariable on changing the deposition temperature of MoO_3. But since the optical band gap energy (E_g) of the MoO_3 thin films decreases from 3.82 ± 0.01 to 3.64 ± 0.01 eV with decreasing deposition temperature, the valence band of the film rises gradually from −5.48 to −5.30 eV, therefore, the potential barrier between FTO and P3HT : PCBM decreases, leading to an increased efficiency with hole injection from P3HT to FTO in an easier way. Thus, the optimized devices have an efficiency of 3.27%, showing a significant improvement of 11.6% in J_{SC} and 20.7% in PCE. It also suggests a key design principle in BHJ solar cells: the buffer layer should have a suitable valence band between the highest occupied molecular orbital of P3HT and the Fermi level of the electrodes as well as a suitable CB, which is higher than the LUMO of P3HT.

4. Conclusion

P3HT : PCBM BHJ solar cells with MoO_3 buffer layers deposited at different substrate temperatures by RF magnetron sputtering are studied. As a result, the PCE of FTO/MoO_3/P3HT : PCBM/Al structure solar cells increases

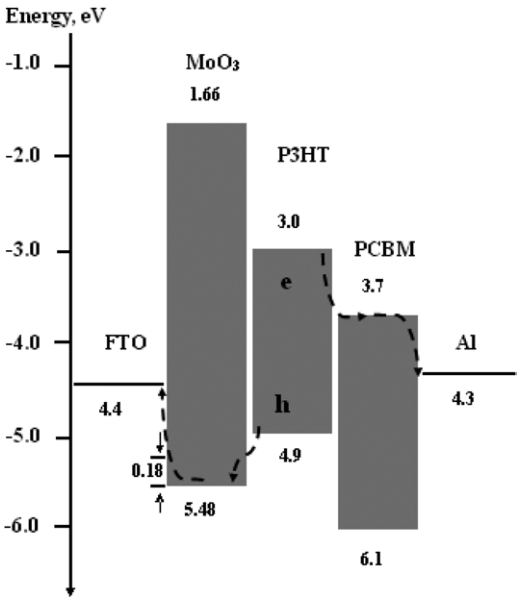

Figure 8. Energy diagram of the FTO/MoO_3/P3HT : PCBM/Al solar cell.

from 2.71% and 3.27% with decreasing substrate temperature from 400 to 100 °C. The structure, morphology, optical and electrical properties of the MoO_3 thin films are investigated. As measured by XRD, the thin films deposited at 300 °C and 400 °C exhibit the presence of monoclinic Mo_9O_{26} and orthorhombic MoO_3, respectively. The optical band gap energy values of the MoO_3 films increase from 3.67 to 3.82 eV with an increase in substrate temperature from 100 to 400 °C. The electrical resistivity values of the MoO_3 thin films are close to each other from 100 to 300 °C and decrease from 2.7×10^6 to 2.6×10^5 Ω cm with increasing substrate temperature from 300 to 400 °C, due to a phase change from monoclinic Mo_9O_{26} to orthorhombic MoO_3. The XPS results show that it is difficult to observe Mo^{4+} and Mo^{5+} states at 100, 300 and 400 °C. Thus, the decrease in the optical band gap of the MoO_3 might have resulted from the rise in the valance band, which decreases the potential barrier between FTO and P3HT : PCBM. Therefore, the efficiency of FTO/MoO_3/P3HT : PCBM/Al structure solar cells is improved from 2.71% to 3.27%, with J_{SC} increasing from 8.51 to 9.50 mA cm^{-2}.

Acknowledgments

This work was supported by the National High Technology Research and Development Program of China (2009AA03Z219), the National Basic Research Program (No 2011CB933300) of China, the National Natural Science Foundation of China (11074194) and the Natural Science Foundation of Jiangsu Province (BK2009143).

References

[1] Shrotriya V, Li G, Yao Y, Chu C W and Yang Y 2006 *Appl. Phys. Lett.* **88** 073508
[2] Kyaw A K K, Sun X W, Jiang C Y, Lo G Q, Zhao D W and Kwong D L 2008 *Appl. Phys. Lett.* **93** 221107
[3] Hori T, Shibata T, Kittichungchit V, Moritou H, Sakai J, Kubo H, Fujii A and Ozaki M 2009 *Thin Solid Films* **518** 522
[4] Kröger M, Hamwi S, Meyer J, Riedl T, Kowalsky W and Kahn A 2009 *Appl. Phys. Lett.* **95** 123301
[5] Meyer J, Shu A, Kröger M and Kahn A 2010 *Appl. Phys. Lett.* **96** 133308
[6] Navas I, Vinodkumar R, Lethy K J, Detty A P, Ganesan V, Sathe V and Mahadevan Pillai V P 2009 *J. Phys. D: Appl. Phys.* **42** 175305
[7] Ramana C V and Julien C M 2006 *Chem. Phys. Lett.* **428** 114
[8] Galatsis K, Li Y and Wlodarski W 2003 *J. Sol–Gel Sci. Technol.* **26** 1097
[9] Liu F, Shao S, Guo X, Zhao Y and Xie Z 2010 *Sol. Energy Mater. Sol. Cells* **94** 842
[10] Lee Y J, Nichols W T, Kim D-G and Kim Y D 2009 *J. Phys. D: Appl. Phys.* **42** 115419
[11] Nirupama V, Gunasekhar K R, Sreedhar B and Uthanna S 2010 *Curr. Appl. Phys.* **10** 272
[12] Uthanna S, Nirupama V and Pierson J F 2010 *Appl. Surf. Sci.* **256** 3133
[13] Uthanna S and Nirupama V 2010 *J. Mater. Sci: Mater. Electron.* **21** 45
[14] Ai L, Fang G J, Yuan L Y, Liu N S, Wang M J, Li C, Zhang Q L, Li J, Zhao X Z 2008 *Appl. Surf. Sci.* **254** 2401
[15] Cullity B D 1956 *Elements of X-ray Diffraction* (Reading, MA: Addison-Wesley)
[16] Anthony S P, Lee J I and Kim J K 2007 *Appl. Phys. Lett.* **90** 103107
[17] Elangovan E, Goncalves G, Martins R and Fortunato E 2009 *Sol. Energy* **83** 726
[18] Navas I, Vinodkumar R, Detty A P, Mahadevan Pillai V P 2009 *IOP Conf. Proc.: Mater. Sci. Eng.* **2** 012035
[19] Miyata N and Akiyoshi S 1985 *J. Appl. Phys.* **58** 1651
[20] Julien C, Khelfa A, Hussain O M and Nazri G A 1995 *J. Cryst. Growth* **156** 235
[21] Li Z P, Gao L and Zheng S 2003 *Mater. Lett.* **57** 4605
[22] Sian T S and Reddy G B 2004 *Sol. Energy Mater. Sol. Cells* **82** 375